

Heterotrimetallic 3d-4d-4f decanuclear metal-capping square showing single-molecule magnet behavior

Jérôme Long, Lise-Marie Chamoreau, Valérie Marvaud*.

Supplementary Information

$[(\text{Mo}(\text{CN})_8)_2(\text{CuLTb})_4](\text{Mo}(\text{CN})_8)$ ($\text{L} = \text{valen}$) noted (1)

$[(\text{Mo}(\text{CN})_8)_2(\text{NiLTb})_4](\text{Mo}(\text{CN})_8)$ ($\text{L} = \text{valen}$) noted (2)

Experimental Section

Crystallographic data for (1) and (2)

Magnetic Properties for (1), (2) and the CuTb dinuclear complex

Experimental Section :

The ligand valen (*N,N'*-bis(3-methoxysalicylidene)ethylenediamine), noted L, was synthesized by reacting one equivalent of ethylenediamine with two equivalents of o-vanillin in ethanol. The bimetallic building block $[\text{CuLTb}](\text{NO}_3)_3$ was synthesized according to the protocol of the literature.^{S1}

$[(\text{Mo}(\text{CN})_8)_2(\text{NiLTb})_4](\text{Mo}(\text{CN})_8)$ (2):

$\text{K}_4[\text{Mo}(\text{CN})_8] \cdot 2\text{H}_2\text{O}$ (0.100 g, 0.201 mmol) dissolved in 10 mL of water was quickly added to a solution of $[\text{NiLTb}](\text{NO}_3)_3$ (0.318g, 0.401 mmol) in 60 mL of $\text{CH}_3\text{CN}/\text{H}_2\text{O}$ 2:1. The solution is stirred for a few seconds before being filtered and let to stand overnight in the dark. Orange needles are then collected. Yield = 22 %

[$\{\text{Mo}(\text{CN})_8\}_2\{\text{NiTbC}_{18}\text{H}_{18}\text{N}_2\text{O}_4(\text{H}_2\text{O})_{3.5}\}_4](\text{Mo}(\text{CN})_8) \bullet 19\text{H}_2\text{O}$ % exp (% calc): Mo 7.67 (7.74), Ni 6.09 (6.31), Tb 18.11 (17.09), C 30.85 (31.00), H 3.57 (3.85), N 12.36 (12.05).

Physical Measurements.

IR spectra were obtained between 4000 and 250 cm^{-1} on a Bio-Rad FTS 165 FT-IR spectrometer on KBr pellets. DC magnetic susceptibility measurements were carried out on a Quantum Design MPMS SQUID susceptometer equipped with a 5 T magnet and operating in the range of temperature from 2 to 400 K. The powdered samples ($10 \pm 50\text{mg}$) were placed in a diamagnetic sample holder and the measurements realised in a 500 Oe applied field using the extraction technique. Before analysis, the experimental susceptibility was corrected from diamagnetism using Pascal constants¹ and from temperature independent paramagnetism (TIP) of the transition metals. AC susceptibility measurements were performed using an oscillating field of 1 Oe and AC frequencies ranging from 1 to 1500 Hz.

Infrared Spectroscopy $[(\text{Mo}(\text{CN})_8)_2(\text{NiLTb})_4](\text{Mo}(\text{CN})_8)$ (2)

The IR spectrum of (2) is similar to the copper analogue and shows several large bands in the cyanide region 2000-2200 cm^{-1} located at 2110, 2122 cm^{-1} and shoulders at 2140 and 2159 cm^{-1} . These bands can be ascribed to the envelope of free cyanide Mo-C≡N and bridged cyanide Mo-C≡N-M respectively. The bands of the valen ligand are found at 1641 and 1607 cm^{-1} ($\nu(\text{C}=\text{N})$ stretching).

X-Ray Crystallography

Suitable crystals for X-ray crystallography were directly obtained from the reaction medium. A single crystal of the compounds was selected rapidly, mounted onto a glass fiber, and transferred in a cold nitrogen gas stream. Intensity data were collected with a Bruker-Nonius Kappa-CCD with graphite-monochromated Mo-K α radiation ($\lambda = 0.71073 \text{ \AA}$). Unit-cell parameters determination, data collection strategy and integration were carried out with the Nonius EVAL-14 suite of programs.³³ The structure was solved by direct methods using the SIR-92 program³⁴ and refined anisotropically by full-matrix least-squares methods using the SHELXL-97 software package (G. M. Sheldrick, University of Göttingen, Germany, 1997).

Single Crystal X-Ray Structure of $[(\text{Mo}(\text{CN})_8)_2(\text{CuLTb})_4](\text{Mo}(\text{CN})_8)$ (1)

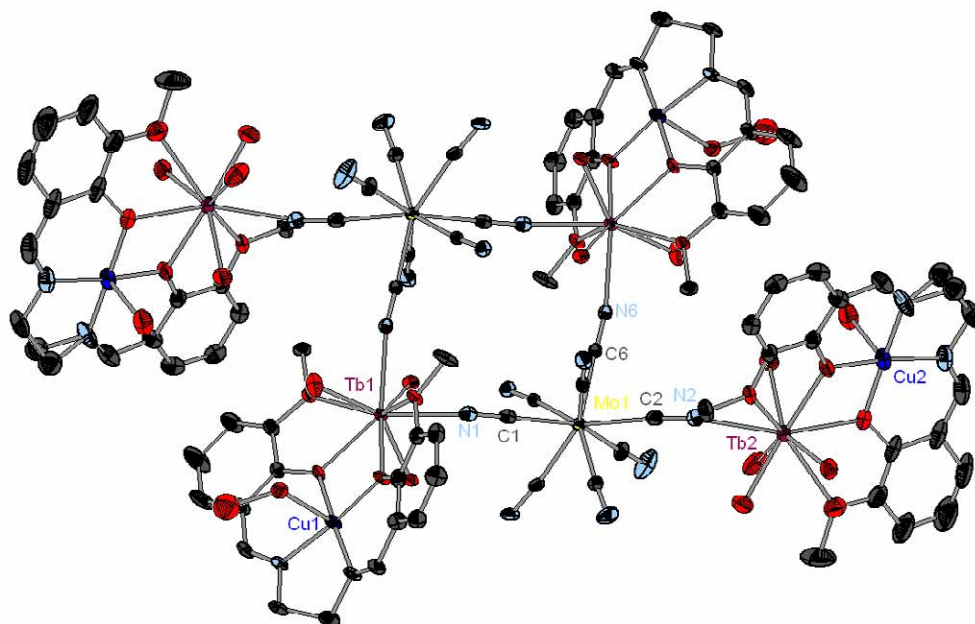


Figure S1. Ortep representation of the X-ray crystal structure of (1)
(thermal ellipsoids set at the 30 % probability level)

Single Crystal X-Ray Structure of $[(\text{Mo}(\text{CN})_8)_2(\text{NiLTb})_4](\text{Mo}(\text{CN})_8)$ (2)

The compound reveals that (2) is isotstructural to the copper equivalent. The compound crystallizes in the monoclinic system, with the $P2_1/c$ space group, the cells parameters being $a = 24.508(3)$ Å, $b = 15.0896(19)$ Å, $c = 19.216(19)$ Å, $\alpha = \gamma = 90^\circ$, $\beta = 108.027(9)^\circ$. The bridging $[\text{NiLTb}]^{3+}$ is connected to two octacyanomolybdate entities with Tb-N distances equal to 2.44 and 2.47 Å. The terminal unit is bridged to one octacyanomolybdate unit with Tb-N distance equal to 2.50 Å.

The Ni-Tb distances are equal to 3.44 Å while the angles of the phenoxo bridge Ni-O-Tb range from 106.61 to 107.33 °.

While the coordination spheres of the terbium is identical to the copper analogue, the nickel ions adopts a square planar geometry.

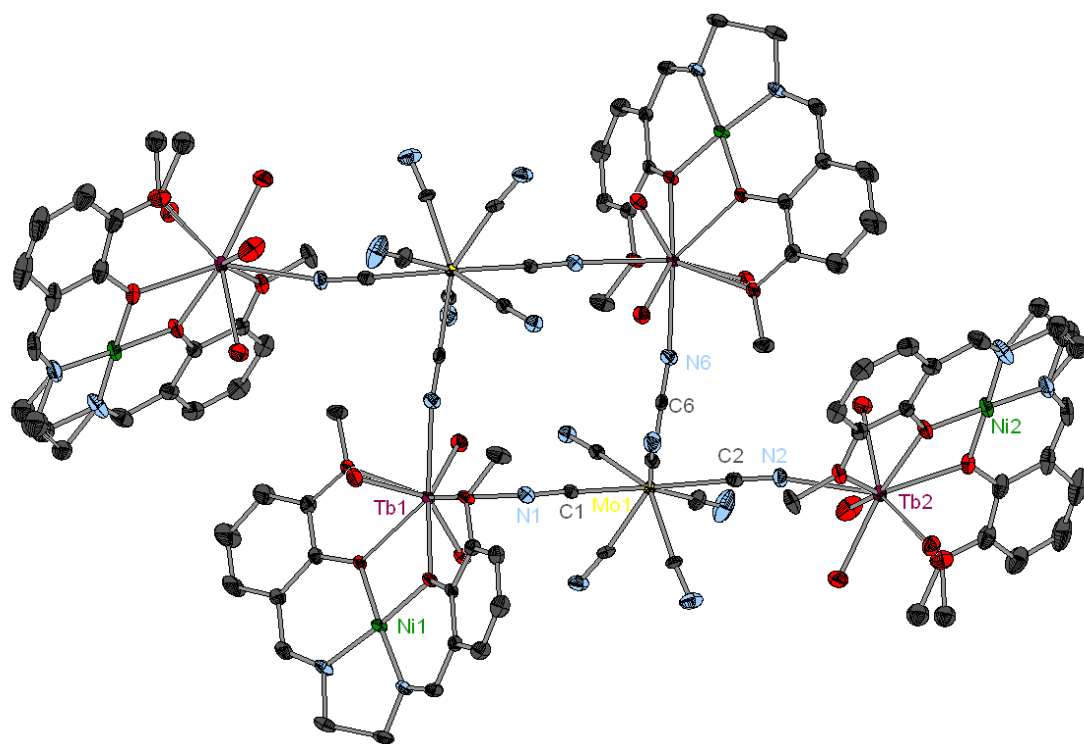
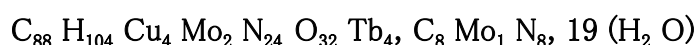


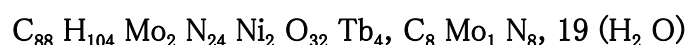
Figure S2. Ortep representation of the X-ray crystal structure of (2)
(thermal ellipsoids set at the 30 % probability level)

Table 1. Crystal data and structure refinement for (1) MoCuTb.



Identification code	jl1240c1		
Empirical formula	C ₉₆ H ₁₄₂ Cu ₄ K ₀ Mo ₃ N ₃₂ O ₅₁ Tb ₄		
Formula weight	3786.08		
Temperature	200(2) K		
Wavelength	0.71073 Å		
Crystal system	Monoclinic		
Space group	P 21/c		
Unit cell dimensions	a = 24.531(3) Å	α= 90° .	
	b = 14.956(2) Å	β= 107.093(11)° .	
	c = 19.283(2) Å	γ= 90° .	
Volume	6762.1(16) Å ³		
Z	2		
Density (calculated)	1.859 Mg/m ³		
Absorption coefficient	3.043 mm ⁻¹		
F(000)	3752		
Crystal size	0.4 x 0.08 x 0.02 mm ³		
Theta range for data collection	2.60 to 27.51° .		
Index ranges	-29≤h≤31, -17≤k≤19, -17≤l≤23		
Reflections collected	40106		
Independent reflections	14005 [R(int) = 0.0747]		
Completeness to theta = 27.51°	90.0 %		
Absorption correction	Semi-empirical from equivalents		
Max. and min. transmission	1 and 0.297		
Refinement method	Full-matrix least-squares on F ²		
Data / restraints / parameters	14005 / 19 / 835		
Goodness-of-fit on F ²	1.011		
Final R indices [I>2sigma(I)]	R1 = 0.0532, wR2 = 0.1163		
R indices (all data)	R1 = 0.1363, wR2 = 0.1423		
Largest diff. peak and hole	1.554 and -1.510 e.Å ⁻³		

Table 2. Crystal data and structure refinement for (2) MoNiTb.



Identification code	jl1362		
Empirical formula	C ₉₆ H ₁₄₂ Mo ₃ N ₃₂ Ni ₄ O ₅₁ Tb ₄		
Formula weight	3718.76		
Temperature	200(2) K		
Wavelength	0.71073 Å		
Crystal system	Monoclinic		
Space group	P 21/c		
Unit cell dimensions	a = 24.508(3) Å	α= 90° .	
	b = 15.0896(19) Å	β= 108.027(9)° .	
	c = 19.2163(19) Å	γ= 90° .	
Volume	6757.6(14) Å ³		
Z	2		
Density (calculated)	1.828 Mg/m ³		
Absorption coefficient	2.970 mm ⁻¹		
F(000)	3696		
Crystal size	0.23 x 0.17 x 0.10 mm ³		
Theta range for data collection	2.23 to 30.01° .		
Index ranges	-34≤h≤34, -20≤k≤21, -27≤l≤27		
Reflections collected	97820		
Independent reflections	19657 [R(int) = 0.1007]		
Completeness to theta = 30.01°	99.5 %		
Absorption correction	Semi-empirical from equivalents		
Max. and min. transmission	0.763 and 0.326		
Refinement method	Full-matrix least-squares on F ²		
Data / restraints / parameters	19657 / 4 / 832		
Goodness-of-fit on F ²	0.986		
Final R indices [I>2sigma(I)]	R1 = 0.0514, wR2 = 0.1174		
R indices (all data)	R1 = 0.1319, wR2 = 0.1471		
Largest diff. peak and hole	1.675 and -2.877 e.Å ⁻³		

Magnetic Properties

The magnetic properties of lanthanide ions are fascinating but they are also well known for their complexity.

Magnetic Properties of $[(\text{Mo}(\text{CN})_8)_2(\text{NiLTb}_4)](\text{Mo}(\text{CN})_8)$ (2)

The magnetic properties are reported on Figure S3. The variation of χT product under a 500 Oe magnetic field shows a continual increase from 300 to 70 K before reaching a maximum at a χT value of $52.07 \text{ cm}^3 \cdot \text{K} \cdot \text{mol}^{-1}$. At room temperature, the χT value of $47.28 \text{ cm}^3 \cdot \text{K} \cdot \text{mol}^{-1}$ is in good agreement with the expected value of $46.71 \text{ cm}^3 \cdot \text{K} \cdot \text{mol}^{-1}$ for four Tb^{III} ions. Below 70 K, the χT product decreases to reach a value of $46.71 \text{ cm}^3 \cdot \text{K} \cdot \text{mol}^{-1}$ at 2 K.

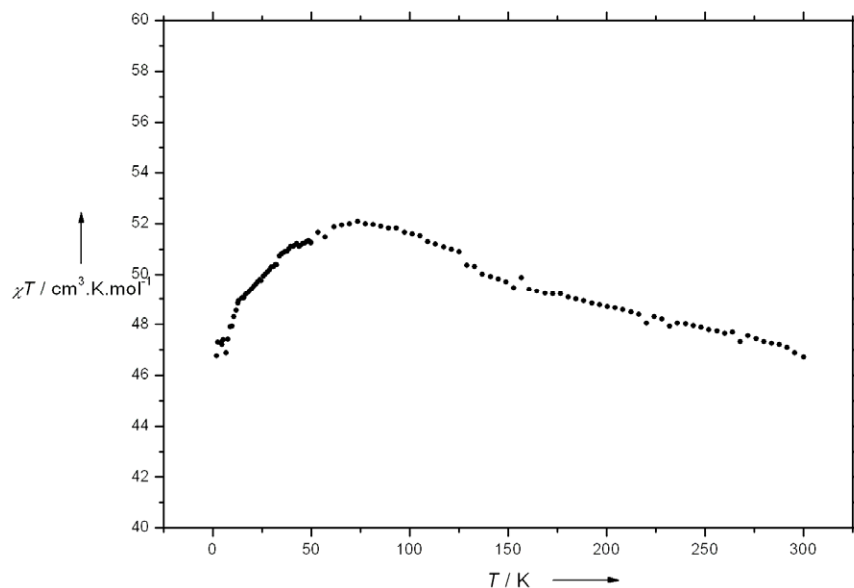


Figure S3: Variation of χT vs. T for (2)

Despite the presence of numerous Tb^{3+} ions, any component of the imaginary susceptibility appears above 2 K, which excludes a single-molecule magnet behavior.

Magnetic Properties of $[(\text{Mo}(\text{CN})_8)_2(\text{CuLTb})_4](\text{Mo}(\text{CN})_8)$ (1)

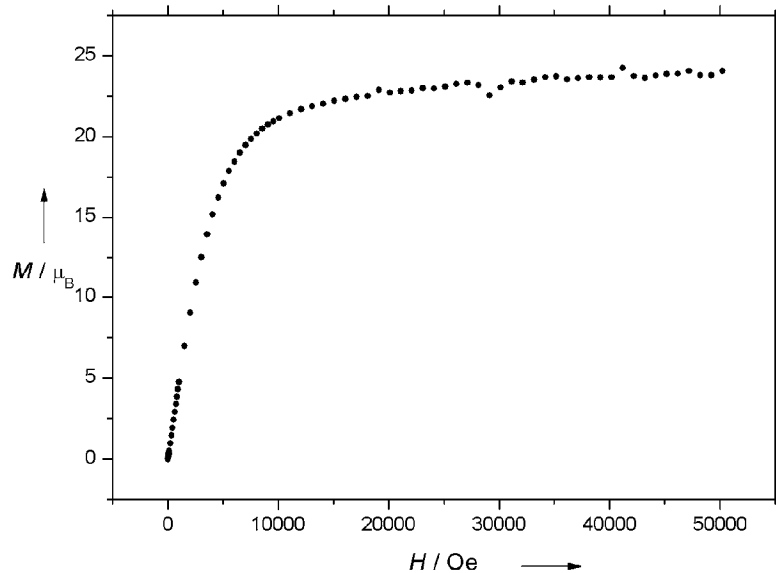


Figure S4. Field dependence of the magnetization recorded at 2K for (1)

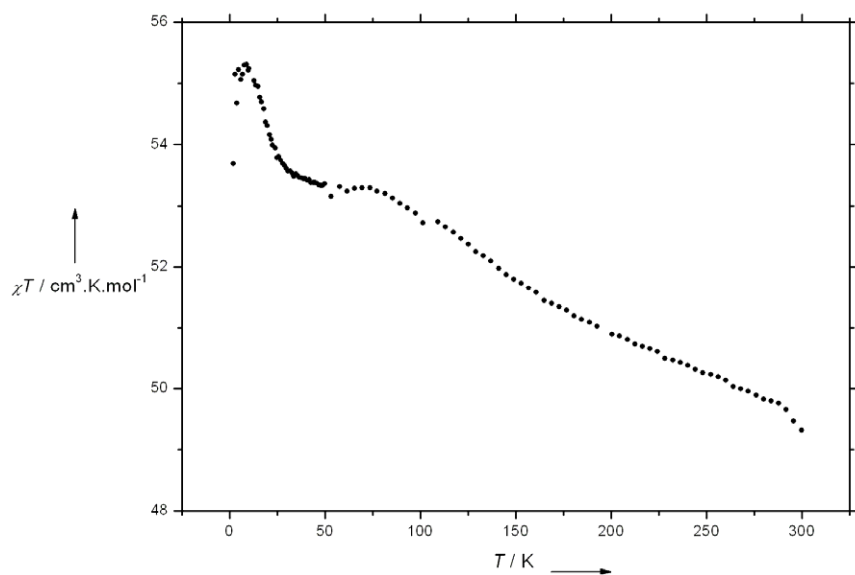


Figure S5. Temperature dependence of the χT values for (1)

The ferromagnetic interaction between the copper and terbium ions can be confirmed by the use of the nickel analogues to evaluate the effect of the ligand field on the lanthanide ion. The representation of $\Delta = \chi_{\text{MoCuTb}} - \chi_{\text{MoNiTb}}$ is shown on **Figure S6**. In the range 50-300 K, Δ remains constant with a value of $2.59 \text{ cm}^3 \cdot \text{K} \cdot \text{mol}^{-1}$. Below 50 K, a positive deviation is observed and can be imputed to ferromagnetic interactions between the copper and terbium ions.

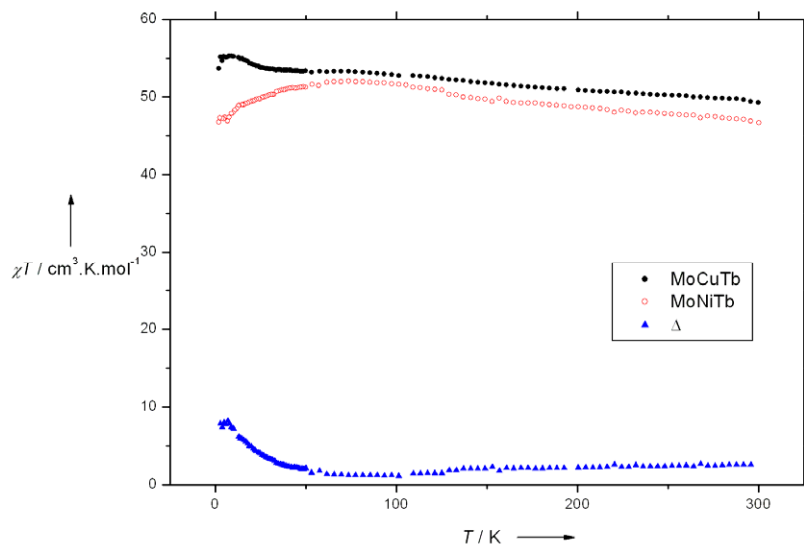


Figure S6: Variation of Δ vs. T

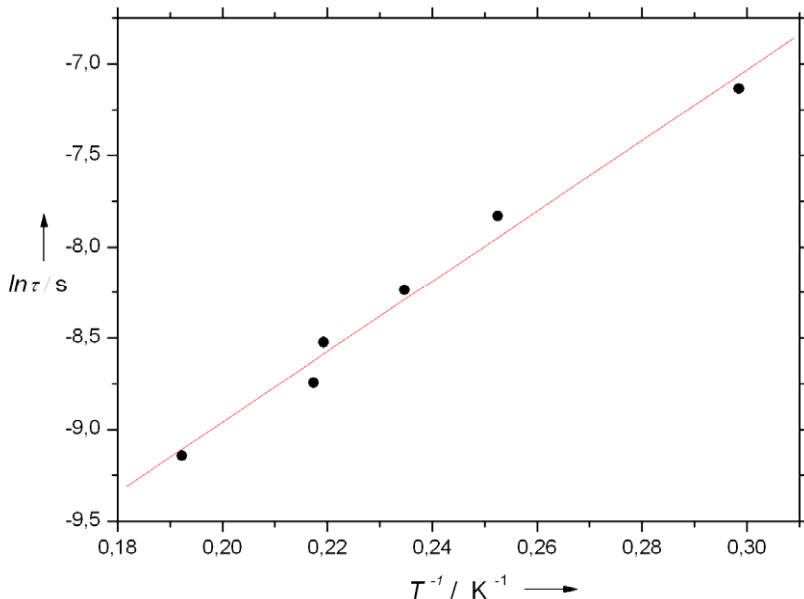


Figure S7: Relaxation time of the magnetization $\ln(\tau)$ vs. T^{-1} (Arrhenius Plot using AC data).

The line corresponds to the fit

Magnetic Properties of the dimer $[\text{CuLTb}]^{3+}$ ($\text{L} = \text{valen}$)

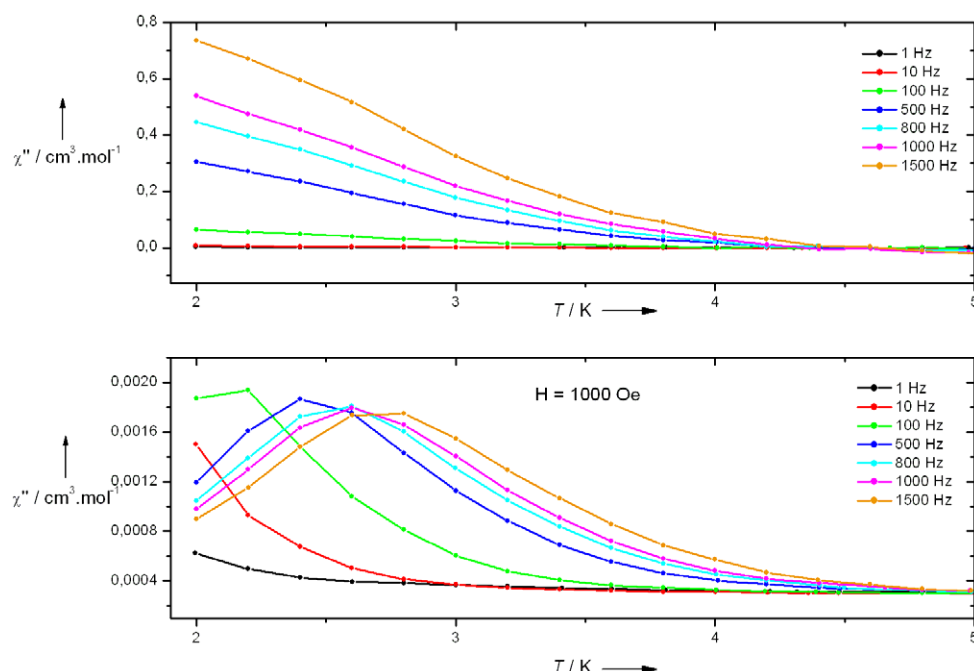


Figure S8. Temperature dependence of the out-of-phase (χ'') ac susceptibility for the dimer $[\text{CuLTb}]^{3+}$ ($\text{L} = \text{valen}$) (top $H = 0$ Oe, bottom $H = 1000$ Oe)

Photomagnetic studies

The photomagnetic experiments do not show any drastic change of the magnetic properties after irradiation with a lamp ($\lambda = 410$ nm). Indeed, the X-ray structure shows clearly that the copper is not directly connected via the cyano-bridge to the molybdenum limiting the possibility of an electron transfer between these two metallic centers through the orbitals of the cyanide. However, it has been shown that for such systems, an outer-sphere electron transfer can occur.^{S2} One can also imagine, an electron transfer from the molybdenum to the copper via the semi-occupied orbitals of the terbium. More recently, we have also demonstrated the feasibility to stabilize Mo(IV) in a high spin configuration, but none of these effect has been observed in the present work and no long lived photo induced metastable state has been evidenced.

References :

- (S1) Costes, J.-P.; Dahan, F.; Dupuis, A.; Laurent, J. *Inorg Chem*, **1996**, *35*, 2400-2402.
(S2) Korzeniak, T.; Mathonière, C.; Kaiba, A.; Guionneau, P.; Koziel, M.; Sieklucka, B. *Inorg. Chim. Acta*, **2008**, *361*, 12-13, 3500-3504.